

## Excitation functions of reactions induced by $^1\text{H}$ and $^2\text{H}$ ions on natural Mg, Al, and Si<sup>†</sup>

R. L. Wilson,\* D. J. Frantsvog,‡ and A. R. Kunselman

*Department of Physics and Astronomy, University of Wyoming, Laramie, Wyoming 82071*

C. Détraz<sup>§</sup>

*Nuclear Physics Laboratory, Department of Physics and Astrophysics, University of Colorado, Boulder, Colorado 80302*

C. S. Zaidins

*Nuclear Physics Laboratory, Department of Physics and Astrophysics, University of Colorado, Boulder, Colorado 80302  
and Department of Physics, University of Colorado, Denver, Colorado 80202*

(Received 8 September 1975)

Cross sections for various reactions induced by beams of  $^1\text{H}$  and  $^2\text{H}$  ions on targets of natural Mg, Al, and Si were determined from observations of the radioactive product  $\gamma$  rays.  $^1\text{H}$  energies between 14.5 and 27.0 MeV and  $^2\text{H}$  energies between 8.7 and 18.0 MeV from the University of Colorado cyclotron were used.

[ NUCLEAR REACTIONS Observed nuclear  $\gamma$  rays, obtained  $\sigma(E_{^1\text{H}})$ ,  $\sigma(E_{^2\text{H}})$  on natural targets Mg, Al, and Si;  $E_{^1\text{H}}=14.5\text{--}27.0$  MeV,  $E_{^2\text{H}}=8.7\text{--}18.0$  MeV. ]

### I. INTRODUCTION

Recent interest<sup>1</sup> in *sd*-shell nuclei has resulted in considerable experimentation<sup>2,3</sup> with these nuclei. Investigators would be aided in designing and optimizing their experiments by accurate measurements of the excitation functions for the various reactions involving the *sd*-shell nuclei. Most of the excitation functions in this region of the chart of nuclides have not been measured and most of those which have been measured have not been measured using contemporary equipment and techniques (see, for example, Ref. 4).

This work, using projectiles of  $^1\text{H}$  and  $^2\text{H}$  over the energy ranges of 14.5 to 27.0 MeV and 8.7 to 14.0 MeV, respectively, and a companion work<sup>5</sup> using projectiles of  $^3\text{He}$  and  $^4\text{He}$  over the energy ranges 10.0 to 41.0 MeV and 10.0 to 37.0 MeV, respectively, are attempts to improve this situation.

### II. EXPERIMENTAL PROCEDURE

Targets of natural magnesium, aluminium, and silicon were irradiated by beams of  $^1\text{H}$  and  $^2\text{H}$  from the University of Colorado 52 in variable energy cyclotron. The beam energies employed were 14.5, 18.8, 22.8, and 27.0 MeV for  $^1\text{H}$  and 8.7, 14.0, and 18.0 MeV for  $^2\text{H}$ . These beam energies were selected from established tunes at the cyclo-

tron facility and the energies checked to confirm that long term energy drifts had not occurred since previous measurements of the tunes.

The projectile energies listed in the tables are corrected for energy loss in an intervening Havar window. Range and energy losses in the windows and targets were calculated using a technique described by Zaidins.<sup>6</sup>

The targets of aluminium and magnesium were prepared from natural foils. The thicknesses of these targets were precisely determined by weighing regular geometric shapes cut from the foils.

The silicon targets were prepared by hand lapping disks of detector grade silicon to the desired thicknesses. These thicknesses were measured in two separate ways. First, the thickness of each target was measured at various places on the disk with precision calipers. Second, the thickness was determined by measuring the diameter of the disk and weighing the disk on a precision balance. In all cases the two methods resulted in very good agreement.

An uncertainty of 10% in the thickness was assigned to all targets. This was considered a conservative estimate and the value of 10% was used in all subsequent calculations.

The targets were moved from the irradiation area inside the cyclotron vault to a well shielded, low background counting area outside the vault by a pneumatic shuttle.<sup>7</sup> The shuttle system had been

recently modified<sup>8</sup> to better accommodate experiments such as this one. Among these improvements was the installation of a Faraday cup<sup>9</sup> which eliminated the necessity of basing the cross sections on the measurement of a calibrating reaction by providing a direct measurement of the beam current. The beam was monitored when the target was in the counting room and an average beam was calculated from an integrated beam current.

Four sequential energy spectra 6.4 sec long were obtained so that the half-lives as well as the energies of the various  $\beta$ -delayed  $\gamma$  rays could be determined. This made identification of the  $\beta$ -decay products more certain.

The spectra were obtained using a well shielded 34 cm<sup>3</sup> cylindrical Ge(Li) detector. Between the target and the detector there was placed 2.54 cm of lucite to attenuate unwanted low energy  $\gamma$  rays and electrons. A Nuclear Data 50-50 multichannel analyzer system was used to store the four spectra. The irradiation and transportation of the target and the counting of  $\beta$ -delayed  $\gamma$  radiation from the target were automatically repeated in a cyclic manner until sufficient data for analysis had been accumulated. Then the run was terminated and the data were transferred electronically into the memory of a PDP-9 computer where preliminary analysis was performed. Each  $\gamma$  peak was fitted to a Gaussian peak with a selected background using a least-squares technique. The peak areas and the peak locations were thus determined.

Energy and efficiency calibrations of the detector were made employing the actual counting ge-

ometry of the experiment. The calibrations were accomplished using sources from the IAEA laboratories and decay information from the paper by Zarnowiecki.<sup>10</sup>

In many cases the final product nucleus could be obtained from several different processes. In such cases the reactions assumed to contribute were those which were energetically more favorable. The results based on these assumptions are presented in the tables. Where possible, absolute cross sections for the formation of a particular product were based on several different  $\gamma$  ray energies and in some cases on the double escape peaks.

The branching ratios and half-lives used in this paper are those reported by Endt and van der Leun<sup>11</sup> except values for  $^{24}\text{Al}$  and  $^{28}\text{P}$  are those reported by Détraz.<sup>12</sup>

The cyclic nature of the experiment precluded the calculation of the absolute cross sections from the experimental data in a straight forward manner. Equation (1) was used to determine the cross sections:

$$\sigma(\text{mb}) = \frac{C \exp(\lambda T_c) M^2 A (T_c - 8S)}{\epsilon B Q X 0.0376 T_c [1 - \exp(-\lambda T_c)]} \times \frac{\exp[(M-1)\lambda T][1 - \exp(\lambda T)]^2}{1 - (M+1)\exp(M\lambda T) + M\exp[(M+1)\lambda T]}, \quad (1)$$

where  $C$  is the total  $\gamma$ -peak area,  $\lambda$  is the decay constant for the  $\gamma$  under investigation;  $M$  is the total number of cycles in the run;  $T_c$  is the total count time per cycle (sec);  $A$  is the gram atomic weight of target material;  $\epsilon$  is the absolute efficiency of the detector at the energy of the  $\gamma$  ray

TABLE I. Absolute cross sections (mb) for the formation of various isotopes resulting from protons incident on natural Mg.

Product	Lab proton beam energy spread within the target				Contributing reactions	Lab threshold energy (MeV)
	13.3-14.0 (MeV)	17.8-18.4 (MeV)	21.9-22.5 (MeV)	26.3-26.7 (MeV)		
$^{21}\text{Na}$	84.5 ± 9.5	61.3 ± 5.8	59.8 ± 6.5	...	$^{24}\text{Mg}(p, ^4\text{He})^{21}\text{Na}$ $^{25}\text{Mg}(p, n ^4\text{He})^{21}\text{Na}$	7.2 14.9
$^{22}\text{Mg}$	...	...	...	0.21 ± 0.11	$^{24}\text{Mg}(p, ^3\text{H})^{22}\text{Mg}$	22.1
$^{23}\text{Mg}$	...	5.2 ± 0.4	40.0 ± 2.9	86.2 ± 6.5	$^{24}\text{Mg}(p, d)^{23}\text{Mg}$ $^{24}\text{Mg}(p, np)^{23}\text{Mg}$ $^{25}\text{Mg}(p, ^3\text{H})^{23}\text{Mg}$ $^{25}\text{Mg}(p, nd)^{23}\text{Mg}$ $^{25}\text{Mg}(p, 2np)^{23}\text{Mg}$	14.9 17.2 16.0 22.6 24.8
$^{24}\text{Na}$	...	1.20 ± 0.09	4.20 ± 0.27	7.31 ± 4.8	$^{25}\text{Mg}(p, 2p)^{24}\text{Na}$ $^{26}\text{Mg}(p, ^3\text{He})^{24}\text{Na}$ $^{26}\text{Mg}(p, pd)^{24}\text{Na}$ $^{26}\text{Mg}(p, 2pn)^{24}\text{Na}$	12.6 16.0 21.7 24.0
$^{24}\text{Al}$	...	7.0 ± 0.5	6.6 ± 0.5	5.1 ± 0.4	$^{24}\text{Mg}(p, n)^{24}\text{Al}$ $^{25}\text{Mg}(p, 2n)^{24}\text{Al}$	15.2 22.8
$^{25}\text{Na}$	...	...	0.64 ± 0.04	1.62 ± 0.11	$^{26}\text{Mg}(p, 2n)^{25}\text{Na}$	14.7

TABLE II. Absolute cross sections (mb) for the formation of various isotopes resulting from protons incident on natural Al.

Product	Lab proton beam energy spread within the target				Contributing reactions	Lab threshold energy (MeV)
	13.5–14.0 (MeV)	18.0–18.4 (MeV)	21.7–22.5 (MeV)	26.0–26.7 (MeV)		
$^{23}\text{Mg}$	0.10 ± 0.07	0.7 ± 0.4	2.9 ± 0.3	10.2 ± 0.9	$^{27}\text{Al}(p, n^4\text{He})^{23}\text{Mg}$	15.5
$^{26}\text{Si}$	...	...	...	0.5 ± 0.1	$^{27}\text{Al}(p, 2n)^{26}\text{Si}$	19.6
$^{27}\text{Si}$	152 ± 15	106 ± 11	42.7 ± 6.5	41.1 ± 7.1	$^{27}\text{Al}(p, n)^{27}\text{Si}$	5.8

being investigated;  $B$  is the branching ratio for the  $\gamma$  of interest expressed as a decimal fraction;  $Q$  is the total charge collected by the Faraday cup (in units of  $10^{10}\text{C}$ );  $X$  is the target thickness ( $\text{mg}/\text{cm}^2$ );  $T_i$  is the total live time of the analyzer for the memory group under consideration;  $T_i = T_1 - 0.511$ , time beam is actually incident on the target in each cycle;  $T$  is the total length of time for one cycle (sec);  $\bar{T} = T_2 + 2GS + \ln\{2\lambda S / [1 - \exp(-2\lambda S)]\} / \lambda$ , time after the beginning of a cycle at which the  $\gamma$  radiation has its "average" value;  $S$  is the multiscalar advance time;  $G$  is the number of the memory group under consideration; and  $T_2$  is the time for the rabbit to move from the irradiation area to the counting area. The development of the cross section equation is presented in detail by Frantsvog.<sup>5</sup>

### III. EXPERIMENTAL RESULTS

The absolute cross sections listed in Tables I–VI are for the formation of the various products

from the naturally occurring isotopic mixtures of the targets. The beam energy spreads listed in the tables result from the degradation of the beam energy in the targets and are expressed in the laboratory system.

In the tables, the contributing reactions were determined by considering all possible channels for the formation of the various products from all of the stable isotopes of the targets and then deleting those which were not energetically possible for the most energetic projectiles used in this experiment. The determinations were made by first calculating the thresholds for each of the reactions using values from Ref. 13 and then converting these energies to the laboratory system to facilitate comparison with the incident beam energies. Cross sections for several products that might have been expected from the energy considerations were not measured.

Measurements of the cross sections for the production of  $^{22}\text{Na}$  from protons and deuterons on

TABLE III. Absolute cross sections (mb) for the formation of various isotopes resulting from protons incident on natural Si.

Product	Lab proton beam energy spread within the target				Contributing reactions	Lab threshold energy (MeV)
	12.9–14.0 (MeV)	17.4–18.4 (MeV)	21.4–22.5 (MeV)	25.8–26.7 (MeV)		
$^{25}\text{Al}$	34 ± 18	55 ± 28	28 ± 14	6.9 ± 3.5	$^{28}\text{Si}(p, ^4\text{He})^{25}\text{Al}$	8.0
$^{27}\text{Si}$	...	38.2 ± 12.0	28.4 ± 2.4	45.5 ± 5.1	$^{28}\text{Si}(p, n^4\text{He})^{25}\text{Al}$	16.7
					$^{28}\text{Si}(p, d)^{27}\text{Si}$	15.5
					$^{28}\text{Si}(p, np)^{27}\text{Si}$	17.8
					$^{29}\text{Si}(p, ^3\text{H})^{27}\text{Si}$	17.8
					$^{29}\text{Si}(p, nd)^{27}\text{Si}$	24.3
$^{28}\text{Al}$	...	0.42 ± 0.03	2.9 ± 0.3	2.3 ± 0.1	$^{29}\text{Si}(p, 2np)^{27}\text{Si}$	26.6
					$^{29}\text{Si}(p, 2p)^{28}\text{Al}$	12.8
					$^{30}\text{Si}(p, ^3\text{He})^{28}\text{Al}$	15.7
					$^{30}\text{Si}(p, pd)^{28}\text{Al}$	21.4
$^{28}\text{P}$	...	6.8 ± 1.0	11.3 ± 1.3	4.3 ± 0.6	$^{30}\text{Si}(p, 2pn)^{28}\text{Al}$	23.7
					$^{28}\text{Si}(p, n)^{28}\text{P}$	15.1
					$^{29}\text{Si}(p, 2n)^{28}\text{P}$	23.8
$^{29}\text{Al}$	...	0.028 ± 0.012	0.31 ± 0.04	0.25 ± 0.04	$^{30}\text{Si}(p, 2p)^{29}\text{Al}$	14.0
$^{29}\text{P}$	0.018 ± 0.002	0.18 ± 0.05	0.36 ± 0.07	0.78 ± 0.33	$^{28}\text{Si}(p, \gamma)^{29}\text{P}$	0.0
					$^{29}\text{Si}(p, n)^{29}\text{P}$	5.9
					$^{30}\text{Si}(p, 2n)^{29}\text{P}$	16.9

TABLE IV. Absolute cross sections (mb) for the formation of various isotopes resulting from deuterons incident on natural Mg.

Product	Lab deuteron beam energy spread within target			Contributing reactions	Lab threshold energy (MeV)
	5.2–7.6 (MeV)	11.8–13.2 (MeV)	16.2–17.3 (MeV)		
$^{24}\text{Na}$	18.2 ± 1.9	24.0 ± 2.0	26.5 ± 2.4	$^{24}\text{Mg}(d, 2p)^{24}\text{Na}$ $^{25}\text{Mg}(d, ^3\text{He})^{24}\text{Na}$ $^{25}\text{Mg}(d, pd)^{24}\text{Na}$ $^{23}\text{Mg}(d, 2pn)^{24}\text{Na}$ $^{26}\text{Mg}(d, ^4\text{He})^{24}\text{Na}$	7.5 7.1 13.1 15.4 0.0
$^{25}\text{Na}$	...	0.52 ± 0.17	0.38 ± 0.05	$^{25}\text{Mg}(d, 2p)^{25}\text{Na}$ $^{26}\text{Mg}(d, ^3\text{He})^{25}\text{Na}$ $^{26}\text{Mg}(d, pd)^{25}\text{Na}$	5.7 9.3 15.2
$^{25}\text{Al}$	290 ± 131	178 ± 20	65 ± 8	$^{24}\text{Mg}(d, n)^{25}\text{Al}$ $^{25}\text{Mg}(d, 2n)^{25}\text{Al}$	0.0 7.8
$^{27}\text{Mg}$	83 ± 10	56 ± 5	22 ± 3	$^{26}\text{Mg}(d, p)^{27}\text{Mg}$	0.0
$^{28}\text{Al}$	0.29 ± 0.06	0.15 ± 0.03	0.03 ± 0.01	$^{26}\text{Mg}(d, \gamma)^{28}\text{Al}$	0.0

magnesium were not undertaken because of the background radiation from  $^{22}\text{Na}$  produced by the cyclotron. All targets were also contaminated to some degree with Na and, therefore, an undetermined contribution to the  $^{22}\text{Na}$  activity from the reaction  $^{23}\text{Na}(p, d)^{22}\text{Na}$  was present.

One might also expect the formation of  $^{26}\text{Al}$  for protons and deuterons on all of the targets but it was not observed. This is attributed to the fact that  $^{26}\text{Al}$  has two isomeric states, one decays by  $\beta$  emission without the emission of  $\gamma$  rays and the other, while it does produce  $\gamma$  rays upon  $\beta$  decay, has a half-life of  $7.4 \times 10^5$  yr, resulting in extremely low intensity radiation. An upper limit on the intensity of the radiation was determined to be 0.01 counts per sec.

The production of  $^{25}\text{Al}$  is energetically possible for protons on all targets and deuterons on targets of Mg and Si. Cross section measurements were not undertaken although, at least in some cases,  $\gamma$  radiation was observed at the proper energies for  $^{25}\text{Al}$ . The observed radiation had a half-life longer than that of  $^{25}\text{Al}$  ( $T_{1/2} = 7.23$  sec) so that a contribution to the activity from  $^{25}\text{Na}$  ( $T_{1/2} = 50$

sec) was suspected. Separation based on the half-lives was not possible because of the extremely low intensity of the radiation.

$^{30}\text{P}$  from protons and deuterons on Si,  $^{27}\text{Si}$  from protons and deuterons on Al and Si, as well as  $^{30}\text{Si}$  from deuterons on Si are all energetically possible but none were observed experimentally. A combination of low cross sections and low branching ratios was probably the cause.

Although  $^{23}\text{Mg}$  was observed in some cases, the reaction  $^{24}\text{Mg}(d, ^3\text{H})^{23}\text{Mg}$  ( $E_{\text{th lab}} = 11.1$  MeV) did not result in measurable radiation for incident deuteron energies up to 17.3 MeV. Since the branching ratio for the 439.9 keV  $\gamma$  ray is 8.7% and the isotopic abundance of  $^{24}\text{Mg}$  is about 79%, one may conclude that the cross section for this reaction must be very low. Calculations indicate the upper limit to be about 1 mb.

Some unexpected products were also observed. For protons of less than 15.5 MeV incident on natural Al, the production of  $^{23}\text{Mg}$  is not expected (see Table II). However, there is a very small cross section with a large uncertainty measured for protons with energies between 13.5 and 14.0

TABLE V. Absolute cross sections (mb) for the formation of various isotopes resulting from deuterons incident on natural Al.

Product	Lab deuteron beam energy spread within target			Contributing reactions	Lab threshold energy (MeV)
	5.9–7.6 (MeV)	11.0–13.2 (MeV)	15.6–17.3 (MeV)		
$^{24}\text{Na}$	...	2.9 ± 0.3	19 ± 1	$^{27}\text{Al}(d, p^4\text{He})^{24}\text{Na}$	5.8
$^{27}\text{Mg}$	...	5.1 ± 0.4	14.6 ± 0.9	$^{27}\text{Al}(d, 2p)^{27}\text{Mg}$	4.4
$^{27}\text{Si}$	...	...	24.1 ± 8.0	$^{27}\text{Al}(d, 2n)^{27}\text{Si}$	8.4
$^{28}\text{Al}$	1000 ± 60	280 ± 20	200 ± 20	$^{27}\text{Al}(d, p)^{28}\text{Al}$	0.0

TABLE VI. Absolute cross sections (mb) for the formation of various isotopes resulting from deuterons incident on natural Si.

Product	Lab deuteron beam energy spread within target			Contributing reactions	Lab threshold energy (MeV)
	2.1-7.6 (MeV)	9.5-13.2 (MeV)	14.3-17.3 (MeV)		
<sup>28</sup> Al	3.0 ± 0.4	15.7 ± 1.7	43.4 ± 4.7	<sup>28</sup> Si( <i>d, 2p</i> ) <sup>28</sup> Al	6.5
				<sup>29</sup> Si( <i>d, <sup>3</sup>He</i> ) <sup>28</sup> Al	7.3
				<sup>29</sup> Si( <i>d, pd</i> ) <sup>28</sup> Al	8.7
				<sup>29</sup> Si( <i>d, 2pn</i> ) <sup>28</sup> Al	15.5
				<sup>30</sup> Si( <i>d, <sup>4</sup>He</i> ) <sup>28</sup> Al	0.0
<sup>29</sup> Al	0.37± 0.09	0.36± 0.05	0.003± 0.001	<sup>29</sup> Si( <i>d, 2p</i> ) <sup>29</sup> Al	5.5
				<sup>30</sup> Si( <i>d, <sup>3</sup>He</i> ) <sup>29</sup> Al	8.5
				<sup>30</sup> Si( <i>d, pd</i> ) <sup>29</sup> Al	14.4
				<sup>30</sup> Si( <i>d, 2pn</i> ) <sup>29</sup> Al	16.8
<sup>29</sup> P	179 ± 25	64 ± 8	81 ± 10	<sup>28</sup> Si( <i>d, n</i> ) <sup>29</sup> P	0.0
				<sup>29</sup> Si( <i>d, 2n</i> ) <sup>29</sup> P	8.5

MeV. A possible explanation might be that the targets were contaminated by Na from the hands of the experimenters yielding the very small amounts of <sup>23</sup>Mg observed at the lower energies from the reaction <sup>23</sup>Na(*p, n*)<sup>23</sup>Mg ( $E_{\text{th lab}} = 5.0$  MeV).

In Table III no cross section is recorded for the lowest beam energy for the production of <sup>29</sup>Al, although low intensity  $\gamma$  radiation was measured and identified to be from <sup>29</sup>Al for these beam energies. This is because the proton energies range from 12.9 to 14.0 MeV in the target and the threshold for the reaction <sup>30</sup>Si(*p, 2p*)<sup>29</sup>Al is 14.0 MeV in the laboratory system. It is thus impossible to determine with a reasonable degree of certainty how much of the target was exposed to protons which had energies above the threshold for the reaction. This precludes the determination of a meaningful cross section for this case.

Due to the rather thick Si targets used, the degradation of the energy of the deuteron beam in the target resulted in the wide energy ranges indicated in Table VI. For the lowest beam energy used this energy spread is from 2.1 to 7.6 MeV. The threshold for the reaction <sup>29</sup>Si(*d, 2p*)<sup>29</sup>Al was calculated to be 5.5 MeV (lab system), thus only about 40% of the target was exposed to deuterons with energies above the threshold for the reaction. Accordingly, in the calculations for this cross section, the target thickness was taken to be 40% of the actual physical thickness.

The information in the tables is presented in such a manner that the interested reader can readily determine more specific information in some cases. For instance, from Table I, <sup>21</sup>Na can be produced from the reactions <sup>24</sup>Mg(*p,  $\alpha$* )<sup>21</sup>Na and <sup>25</sup>Mg(*p, n $\alpha$* )<sup>21</sup>Na over the energy range investigated. Indeed, most of the cross sections recorded probably represent contributions from both

reactions; however, for the lowest beam energy, only the former reaction can contribute. Equation (2) takes into proper account the isotopic abundance of the target isotope <sup>24</sup>Mg ( $I_{\text{AB}} = 0.79$ ) so that the absolute cross section for the specific reaction <sup>24</sup>Mg(*p,  $\alpha$* )<sup>21</sup>Na can be found to be (107 ± 12) mb over the energy range 13.3 to 14.0 MeV.

$$\sigma_{\text{iso}} = (1/I_{\text{AB}})\sigma_{\text{nat}}, \quad (2)$$

where  $\sigma_{\text{iso}}$  is the cross section for the formation of the particular isotope,  $I_{\text{AB}}$  is the isotopic abundance of the isotope in the naturally occurring element expressed as a decimal, and  $\sigma_{\text{nat}}$  is the cross section for the formation of the product from the natural element.

#### IV. DISCUSSION AND CONCLUSIONS

Absolute cross sections for the reaction <sup>25</sup>Mg(*p, 2p*)<sup>24</sup>Na have been measured by Cohen, Reynolds, and Zucker<sup>14</sup> and by Meadows and Holt.<sup>15</sup> Meadows and Holt used a separated target, whereas Cohen *et al.* used natural Mg. A comparison of the present work thus can easily be made with the results of Cohen *et al.* by using formula (2) to find the cross sections for the target isotope <sup>25</sup>Mg. The resulting agreement is good and is shown in Fig. 1. The differences between the results of Meadows and Holt and Cohen *et al.* appear to be due to the reaction <sup>26</sup>Mg(*p, <sup>3</sup>He*)<sup>24</sup>Na. A subtraction of the cross sections found by Meadows and Holt from those reported by Cohen *et al.* could be used to determine cross sections for the reaction <sup>26</sup>Mg(*p, <sup>3</sup>He*)<sup>24</sup>Na. The information presented in this work could be used in a similar manner to extend the determinations to higher beam energies than were used by Cohen *et al.* From a cursory examination it appears that the uncertainties involved should be of

the order of 30%.

A comparison of the results of this work and those of Cohen<sup>16</sup> for the reaction  $^{29}\text{Si}(p, 2p)^{28}\text{Al}$  can be made by assuming that the only contributing target isotope is  $^{29}\text{Si}$  and converting the cross sections given in Table III according to equation (2). This has been done and the results are presented in Fig. 2.

Cohen used an enriched target and claimed good reproducibility for his results which would refute any possibility of a nonuniform target thickness. The targets used here were of natural Si of well established thicknesses. The use of natural targets allows the possibility of  $^{30}\text{Si}(p, ^3\text{He})^{28}\text{Al}$  contributing to the activity, which was assumed to be entirely from the reaction  $^{29}\text{Si}(p, 2p)^{28}\text{Al}$ . If the former reaction did contribute, the corrected cross sections would be smaller than those presented in Fig. 2 resulting in poorer agreement.

The threshold for the  $^{29}\text{Si}(p, 2p)^{28}\text{Al}$  reaction is 12.8 MeV (lab) and the proton Coulomb barrier is about 5.1 MeV, hence one would not expect an appreciable cross section until the proton beam en-

ergy is well above 12 MeV. This energy is more consistent with the present work than with the results of Cohen. A further consideration can be made by comparing the excitation functions found here and by Cohen to the excitation function of a similar reaction. The reaction  $^{30}\text{Si}(p, 2p)^{29}\text{Al}$  might be considered such a similar reaction. This excitation function and that found for the production of  $^{28}\text{Al}$  in the present work agree favorably in both energy dependence and magnitude when the isotopic abundances are taken into account while the excitation function for the same reaction found by Cohen differs significantly. A study of Cohen's paper gives no indication as to why this discrepancy exists. Likewise, a careful study of the present work indicates no reason to suspect that the results reported here might be invalid.

The  $^{27}\text{Al}(d, p\alpha)^{24}\text{Na}$  excitation function has been measured by Clarke<sup>17</sup> and Batzel, Crane, and O'Kelley,<sup>18</sup> and the present authors and the results of all three works are given in Fig. 3. The three works are in fair agreement. Both Clarke and Batzel *et al.* used  $\beta$ -counting techniques. All three works are consistent with the observation that

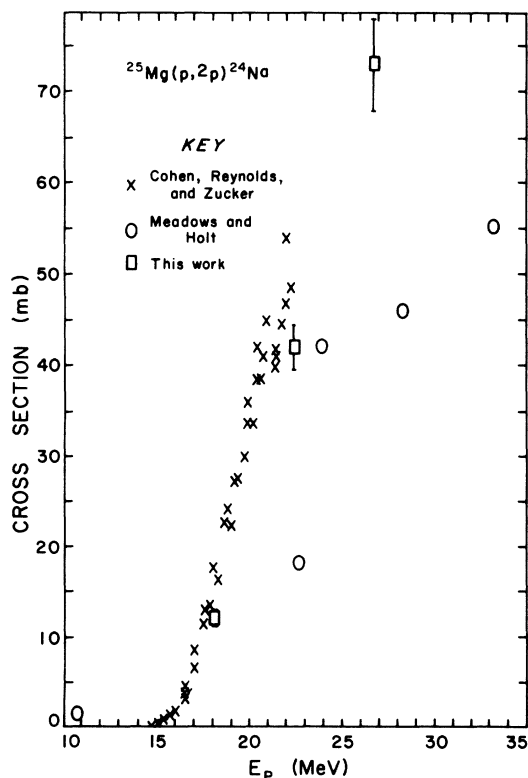


FIG. 1. A comparison of the excitation functions obtained by Cohen *et al.* (Ref. 14), Meadows and Holt (Ref. 15), and this work for the reaction  $^{25}\text{Mg}(p, 2p)^{24}\text{Na}$ . The reaction  $^{26}\text{Mg}(p, ^3\text{He})^{24}\text{Na}$  is assumed to be ignorable.

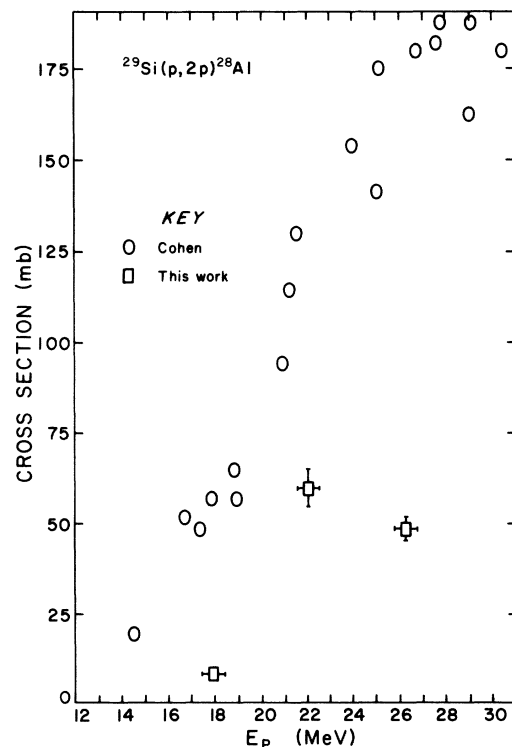


FIG. 2. A comparison of the excitation functions obtained by Cohen (Ref. 16) and this work for the reaction  $^{29}\text{Si}(p, 2p)^{28}\text{Al}$ . The reaction  $^{30}\text{Si}(p, ^3\text{He})^{28}\text{Al}$  is assumed to be ignorable.

because of the threshold and the Coulomb barrier, very low cross sections should be observed below about 10.2 MeV.

No correction was made in this paper for the knock-on neutron-induced  $^{27}\text{Al}(n, \alpha)^{24}\text{Na}$  reaction because of the thin target assumption. Clarke used the stacked foil method and found it necessary to make this correction.

The thin target assumption may be subject to some doubt in this case as is shown graphically in Fig. 3 by the wide range of proton energies within the target. Clarke's paper attributes nearly 30% of the activity produced at deuteron energies of 11 MeV to the capture of neutrons produced by the incident deuteron beam.

Na is among the contaminants of the natural Al targets used in this experiment, and some contribution to the cross sections at the lower energies is expected from the  $^{23}\text{Na}(d, p)^{24}\text{Na}$  reaction which could not be corrected for.

Figure 4 compares the results of this work with Radicella *et al.*<sup>19</sup> for the reaction  $^{27}\text{Al}(d, 2p)^{27}\text{Mg}$  for beam energies up to 18 MeV. Radicella *et al.* measured the  $\beta$  activity over a period of several days in order to be able to separate the contribu-

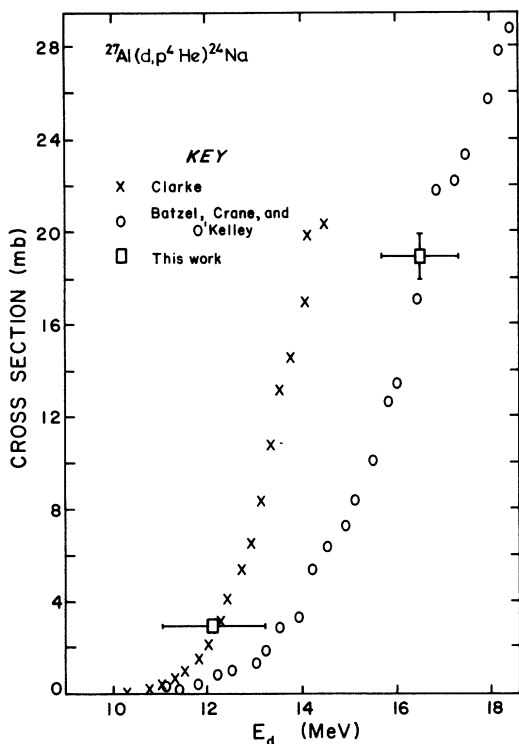


FIG. 3. A comparison of the excitation functions obtained by Clarke (Ref. 17), R. E. Batzel *et al.* (Ref. 18) and this work for the reaction  $^{27}\text{Al}(d, p^4\text{He})^{24}\text{Na}$ .

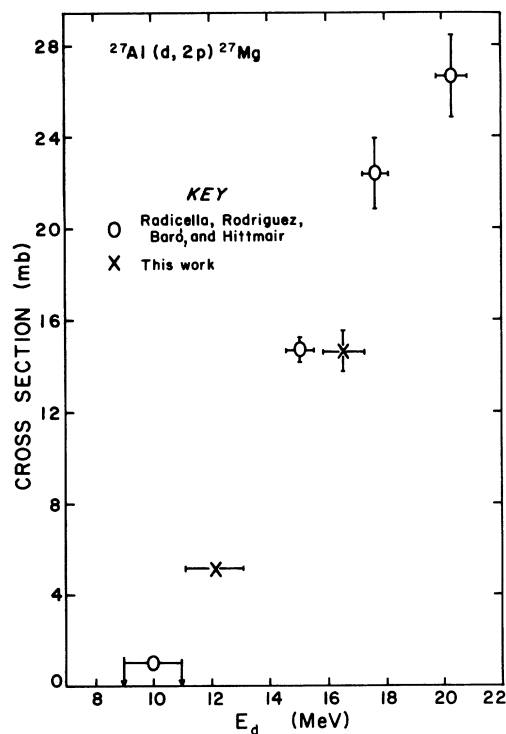


FIG. 4. A comparison of the excitation functions obtained by Radicella *et al.* (Ref. 19) and this work for the reaction  $^{27}\text{Al}(d, 2p)^{27}\text{Mg}$ .

tions made by  $^{24}\text{Na}(T_{1/2} = 15 \text{ h})$  and  $^{27}\text{Mg}(T_{1/2} = 9.5 \text{ min})$ . The resulting activities were then extrapolated back to give the activities at the end of the irradiation period. The cross sections for the formation of  $^{27}\text{Mg}$  were calculated using the cross sections and activities for the reaction  $^{27}\text{Al}(d, p\alpha)^{24}\text{Na}$  found by Batzel *et al.*<sup>18</sup> for normalization. A small discrepancy between the cross section found by Radicella *et al.* and that found in the present work exists for the beam energy of 18 MeV. However, for the beam energy of 18 MeV, the agreement between the present authors and Batzel *et al.* for the  $^{27}\text{Al}(d, p^4\text{He})^{24}\text{Na}$  reaction, upon which the work of Radicella *et al.* is based, is excellent (Fig. 3). Since the measurements in this work for both the  $^{24}\text{Na}$  and the  $^{27}\text{Mg}$  were made in an identical manner, the  $^{24}\text{Na}$  agreement with Batzel *et al.* implies substantiation of the cross sections calculated for  $^{27}\text{Mg}$  as well. The small difference between this work and that of Radicella is probably due to the extrapolation or separation processes of Radicella.

We would like to express our appreciation to L. Erb, D. Zurstadt, Dr. H. Fielding, Dr. C. Moss, B. Phillips, J. L. Homan, and the cyclotron staff.

†Work supported in part by the U.S. ERDA.

\*Present address: Northern Nevada Community College, Elko, Nevada 89801.

‡Present address: Institute de Physique Nucleaire, B.P. 1, 91-Orsay, France.

§Present address: Concordia College, Moorhead, Minnesota 56560.

<sup>1</sup>D. R. Goosman, K. W. Jones, E. K. Warburton, and D. E. Alburger, *Phys. Rev. C* **4**, 1800 (1971).

<sup>2</sup>C. E. Moss, C. Détraz, and C. S. Zaidins, *Nucl. Phys. A* **174**, 408 (1971); *A* **170**, 111 (1971); C. Détraz, C. E. Moss, and C. S. Zaidins, *Phys. Lett.* **34B**, 128 (1971).

<sup>3</sup>C. Détraz *et al.*, *Nucl. Phys. A* **203**, 414 (1973).

<sup>4</sup>D. B. Smith, Los Alamos Scientific Laboratory Report No. LA-2424, 1960 (unpublished).

<sup>5</sup>D. J. Frantsvog (unpublished).

<sup>6</sup>C. S. Zaidins, *Nucl. Instrum. Methods* **120**, 125 (1974).

<sup>7</sup>W. C. Anderson, Ph.D. thesis, University of Colorado, 1964 (unpublished).

<sup>8</sup>M. J. Fritts and C. S. Zaidins, University of Colorado

Report, 1974 (unpublished).

<sup>9</sup>R. L. Wilson, Ph.D. thesis, University of Wyoming, 1975 (unpublished).

<sup>10</sup>K. Zarnowiecki, *Nucl. Instrum. Methods* **55**, 329 (1967).

<sup>11</sup>P. M. Endt and C. van der Leun, *Nucl. Phys. A* **214**, 1 (1973).

<sup>12</sup>C. Détraz, *Nucl. Phys. A* **188**, 513 (1972).

<sup>13</sup>C. M. Lederer, J. M. Hollander, and I. Perlman, *Table of Isotopes* (Wiley, New York, 1968), 6th ed.

<sup>14</sup>B. L. Cohen, H. L. Reynolds, and A. Zucker, *Phys. Rev.* **96**, 1617 (1954).

<sup>15</sup>J. W. Meadows and R. B. Holt, *Phys. Rev.* **83**, 47 (1951).

<sup>16</sup>L. Cohen, *Phys. Rev.* **102**, 453 (1956).

<sup>17</sup>E. T. Clarke, *Phys.* **71**, 187 (1947).

<sup>18</sup>R. E. Batzel, W. W. T. Crane, and G. D. O'Kelley, *Phys. Rev.* **91**, 939 (1953).

<sup>19</sup>R. Radicella, J. Rodriguez, G. B. Baro', and O. Hittmair, *Z. Phys.* **150**, 653 (1958).